

# Strange hadron production in pp, pPb and PbPb collisions at LHC energies

Kapil Saraswat<sup>1</sup>, Prashant Shukla<sup>2,3,a</sup>, Vineet Kumar<sup>2</sup>, and Venktesh Singh<sup>1</sup>

<sup>1</sup> Department of Physics, Institute of Science, Banaras Hindu University, Varanasi 221005, India

<sup>2</sup> Nuclear Physics Division, Bhabha Atomic Research Center, Mumbai 400085, India

<sup>3</sup> Homi Bhabha National Institute, Anushakti Nagar, Mumbai 400094, India

Received: 12 September 2016 / Revised: 5 April 2017

Published online: 8 May 2017 – © Società Italiana di Fisica / Springer-Verlag 2017

Communicated by G. Torrieri

**Abstract.** We present a systematic analysis of transverse momentum ( $p_T$ ) spectra of the strange hadrons in different multiplicity events produced in pp collision at  $\sqrt{s} = 7$  TeV, pPb collision at  $\sqrt{s_{NN}} = 5.02$  TeV and PbPb collision at  $\sqrt{s_{NN}} = 2.76$  TeV. Both the single and differential freeze-out scenarios of strange hadrons  $K_s^0$ ,  $\Lambda$  and  $\Xi^-$  are considered while fitting using a Tsallis distribution which is modified to include transverse flow. The  $p_T$  distributions of these hadrons in different systems are characterized in terms of the parameters, namely Tsallis temperature ( $T$ ), power ( $n$ ) and average transverse flow velocity ( $\beta$ ). It is found that for all the systems, transverse flow increases as we move from lower to higher multiplicity events. In the case of the differential freeze-out scenario, the degree of thermalization remains similar for events of different multiplicity classes in all the three systems. The Tsallis temperature increases with the mass of the hadrons and also increases with the event multiplicity in pp and pPb system but shows little variation with the multiplicity in PbPb system. In the case of the single freeze-out scenario, the difference between small systems (pp, pPb) and PbPb system becomes more evident. The high-multiplicity PbPb events show higher degree of thermalization as compared to the events of pp and pPb systems. The trend of variation of the temperature in PbPb system with event multiplicity is opposite to what is found in the pp and pPb systems.

## 1 Introduction

The heavy ion collisions at RHIC and LHC aim to create matter with high energy density required for the formation of Quark Gluon Plasma (QGP) [1–3]. The quark gluon matter once formed, presumably with local thermal equilibrium expands, cools and undergoes a phase transition to hadronic matter. The hadronic matter continues to expand and once the mean free path of hadrons becomes bigger than the system size, they decouple from the system and move to the detectors. The transverse momentum ( $p_T$ ) spectra of hadrons reflect the condition of the system at the time of freeze-out. The  $p_T$  spectra of hadrons such as pions, kaons, protons and strange baryons have been a very useful tool to study particle production mechanisms, thermalization and collective effects in a large system [4, 5]. At LHC, three different types of collisions: proton-proton (pp), proton-lead (pPb), and lead-lead (PbPb) are performed at different center-of-mass energies.

The nucleus at high energy is considered to be a system of very dense partons. These partons can undergo simul-

taneous and independent scatterings during initial collisions and produce large number of particles in the final state. The thermalization time scale commonly assumed for the QGP created in nuclear collisions is significantly less than 1 fm/c [6] which is small compared to the size of a heavy nucleus and thus it is expected that the system thermalizes. There have been discussions of collectivity [7] in pp collisions also, after the observation of long-range rapidity correlations in high-multiplicity pp events at LHC energy [8]. A Boltzmann-Gibbs blast wave model fit has been performed on strange and non-strange hadrons produced in pp collisions in ref. [9] concluding that there is a collective transverse flow in small systems.

The Tsallis distribution [10, 11] describes near thermal systems in terms of two parameters, temperature  $T$  and parameter  $q$  which measures temperature fluctuation or degree of non-thermalization. It is known [12, 13] that the functional form of the Tsallis distribution with thermodynamic origin in terms of the parameter  $q$  is the same as the QCD-inspired Hagedorn formula in terms of the parameter  $n$  [14, 15]. The parameter  $n$  or  $q$  governs the power law tail of the  $p_T$  spectra. The Tsallis function gives an excellent description of  $p_T$  spectra of all identified mesons

<sup>a</sup> e-mail: pshukla@barc.gov.in

measured in pp collisions at RHIC and LHC energies [12, 16, 17]. The hadron  $p_T$  distributions in heavy ion collisions are modified due to collective flow so the Tsallis blast wave method is used as in ref. [18]. The average transverse flow is included in the Tsallis distribution in ref. [19] keeping the functional form analytical. This modified function can be used in a wider  $p_T$  range as was done for both meson and baryon spectra in heavy ion collisions at RHIC and LHC [19, 20]. A Tsallis analysis of  $p_T$  spectra of identified particles produced in pp collisions at various RHIC and LHC energies has been performed in ref. [21].

The ALICE experiment has measured identified charged hadron spectra in PbPb collisions at  $\sqrt{s_{NN}} = 2.76$  TeV for many centrality classes [22]. They have also carried out a combined blast wave analysis of all particle spectra in a single freeze-out scenario choosing an intermediate  $p_T$  range where hydrodynamics is assumed to be applicable. They obtained inverse slope parameter of blast wave function in chosen fit-ranges of particle spectra. Few analyses perform fits in terms of different sets of parameters for strange and non-strange particles [20]. There are recent analyses of LHC data [23–25] suggesting a differential freeze-out scenario for different particles. The Tsallis study of  $p_T$  spectra in pp and AA collisions in ref. [24] finds heavier particles freeze-out at higher temperatures. They also carried out a blast wave analysis to obtain radial flow of particles. The work in refs. [24, 25] analyses the  $p_T$  spectra of  $\pi^+$ ,  $K^+$ ,  $p$ ,  $d$  and  ${}^3\text{He}$  particles in PbPb collisions at  $\sqrt{s_{NN}} = 2.76$  TeV using the Tsallis distribution in different centralities. The extracted temperature is found to increase with the increase of the particle rest mass. The intercept in temperature and mass correlation has been regarded as the mean kinetic freeze-out temperature of the system. The higher effective temperature in the central collisions as compared to that in the peripheral collisions is attributed to the higher excitation state of the system in central collisions at the time of freeze-out [25]. The transverse flow velocity of the produced particles in the source rest frame is extracted based on the slopes in the linear relation between the mean  $p_T$  and mean moving mass.

In this work, we use the Tsallis distribution with transverse flow to carry out the analysis of  $p_T$  spectra of strange hadrons in different multiplicity events produced in pp collision at  $\sqrt{s} = 7$  TeV, pPb collision at  $\sqrt{s_{NN}} = 5.02$  TeV and PbPb collision at  $\sqrt{s_{NN}} = 2.76$  TeV. We perform the fits of spectra of strange hadrons  $K_s^0$ ,  $\Lambda$  and  $\Xi^-$  considering both single and differential freeze-out scenarios. The ( $p_T$ ) distributions of these hadrons in different systems are characterized in terms of the parameters, namely Tsallis temperature ( $T$ ), power ( $n$ ) and average radial flow velocity ( $\beta$ ). The goal is to study the behaviour of the three systems with two different freeze-out scenarios.

## 2 Tsallis distribution function with transverse flow

The transverse momentum spectra of hadrons can be described using the modified Tsallis distribution [19]. The

modified Tsallis function is given by

$$E \frac{d^3N}{dp^3} = C_n \left[ \exp \left( \frac{-\gamma \beta p_T}{nT} \right) + \frac{\gamma m_T}{nT} \right]^{-n}. \quad (1)$$

Here  $C_n$  is the normalization constant,  $m_T(\sqrt{p_T^2 + m^2})$  is the transverse mass,  $\gamma = 1/\sqrt{1 - \beta^2}$ ,  $\beta$  is the average transverse velocity of the system and  $T$  is the temperature. The power  $n$  is related to the Tsallis parameter  $q$  as  $n = 1/(q - 1)$ , where  $q$  gives temperature fluctuations [26] in the system as  $q - 1 = \text{Var}(T)/\langle T \rangle^2$ . The parameter  $n$  can be called degree of thermalization [26]. Larger values of  $n$  correspond to smaller values of  $q$ . Both  $n$  and  $q$  have been interchangeably used in the Tsallis distribution [11, 16, 27–29]. The Tsallis interpretation of parameters  $T$  as temperature and  $q$  as non-extensivity parameter is more suited for heavy ion collisions while for pp collisions Hagedorn interpretation in terms of power  $n$  and inverse slope parameter  $T$  is more meaningful. Phenomenological studies suggest that, for quark-quark point scattering,  $n \sim 4$  [30, 31], and when multiple scattering centers are involved  $n$  grows larger.

When  $\beta$  is zero, eq. (1) is the usual Tsallis equation

$$E \frac{d^3N}{dp^3} = C_n \left( 1 + \frac{m_T}{nT} \right)^{-n}. \quad (2)$$

In recent years, Tsallis distribution has been the most popular tool to characterize hadronic collisions [13, 26, 27, 32]. At low  $p_T$ , eq. (1) represents a thermalized system with collective flow

$$E \frac{d^3N}{dp^3} \simeq C_n \exp \left( \frac{-\gamma(m_T - \beta p_T)}{T} \right) \quad \text{for } p_T \rightarrow 0. \quad (3)$$

At high  $p_T$ , it becomes a power law

$$E \frac{d^3N}{dp^3} \simeq C_n \left( \frac{\gamma m_T}{nT} \right)^{-n} \quad \text{for } p_T \rightarrow \infty. \quad (4)$$

For very large  $n$  ( $\rightarrow \infty$ ) (or  $q \rightarrow 1$ ), eq. (1) takes the Boltzmann form with transverse flow as in eq. (3).

## 3 Results and discussions

In the present analysis, we use  $p_T$  spectra of the strange hadrons produced in different multiplicity events of pp collision at  $\sqrt{s} = 7$  TeV, pPb collision at  $\sqrt{s_{NN}} = 5.02$  TeV and PbPb collision at  $\sqrt{s_{NN}} = 2.76$  TeV measured by CMS experiment [33]. The measured  $p_T$  spectra of  $K_s^0$ ,  $\Lambda$  and  $\Xi^-$  particles are fitted with the modified Tsallis distribution (eq. (1)) using two methods. First, we assume a differential freeze-out scenario and analyse the  $p_T$  spectra of  $K_s^0$ ,  $\Lambda$  and  $\Xi^-$  individually. In the second method, we assume a single freeze-out scenario and perform a combined fitting of all the three hadron spectra simultaneously in each multiplicity bin.

Figure 1 shows the invariant yields of the strange hadrons ((a)  $K_s^0$ , (b)  $\Lambda$  and (c)  $\Xi^-$ ) as a function of  $p_T$

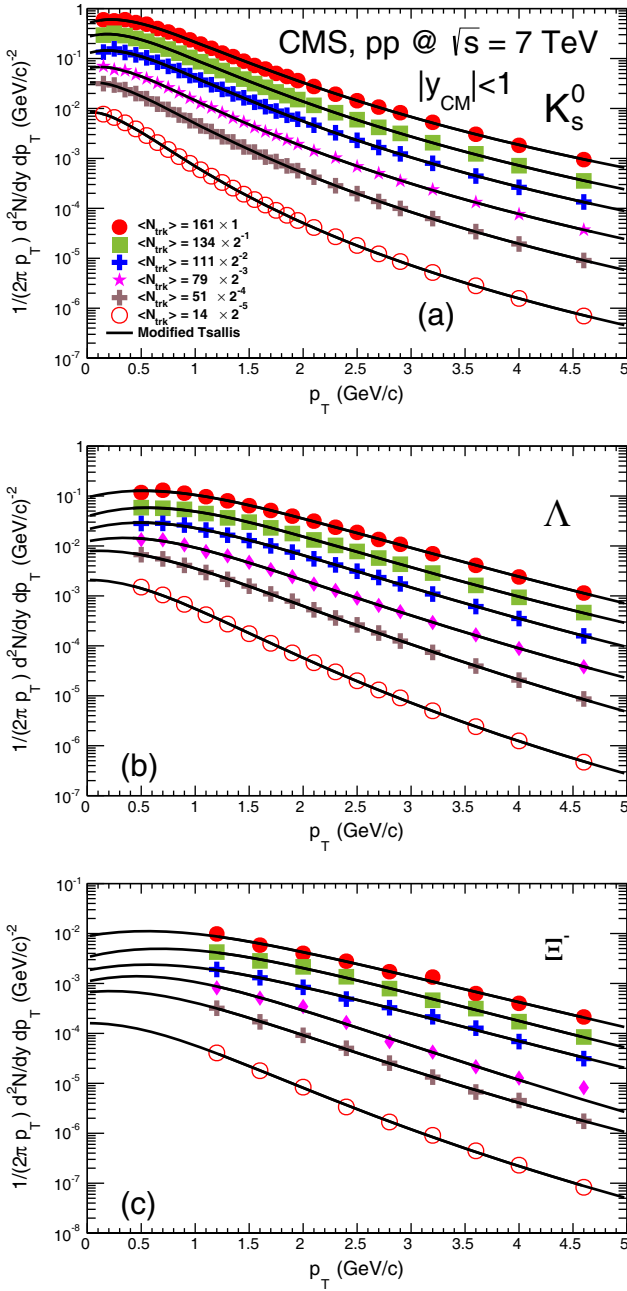


**Fig. 1.** The invariant yields of the  $K_s^0$ ,  $\Lambda$  and  $\Xi^-$  hadrons as a function of the transverse momentum  $p_T$  for pp collisions at  $\sqrt{s} = 7$  TeV measured by CMS [33]. The yields are shown for different multiplicity bins. The solid curves are the fitted modified Tsallis distribution.

for pp collisions at  $\sqrt{s} = 7$  TeV measured by the CMS experiment [33] in the mid rapidity,  $|y_{CM}| < 1$ . The invariant yields are given for six multiplicity classes which correspond to the efficiency corrected average track multiplicities  $\langle N_{\text{trk}} \rangle = 14, 51, 79, 111, 134$  and  $161$ . The solid curves are the modified Tsallis distributions fitted individually to different hadron spectra. The individual fitting gives excellent fit quality for all the multiplicity classes

**Table 1.**  $\chi^2/\text{NDF}$  of the strange hadrons production in pp collision at  $\sqrt{s} = 7$  TeV obtained using individual fitting.

$\langle N_{\text{trk}} \rangle$	$\chi^2/\text{NDF}$		
	$K_s^0$	$\Lambda$	$\Xi^-$
14	0.022	0.106	0.198
51	0.013	0.062	0.150
79	0.049	0.092	0.439
111	0.061	0.047	0.206
134	0.033	0.035	0.138
161	0.063	0.063	0.388

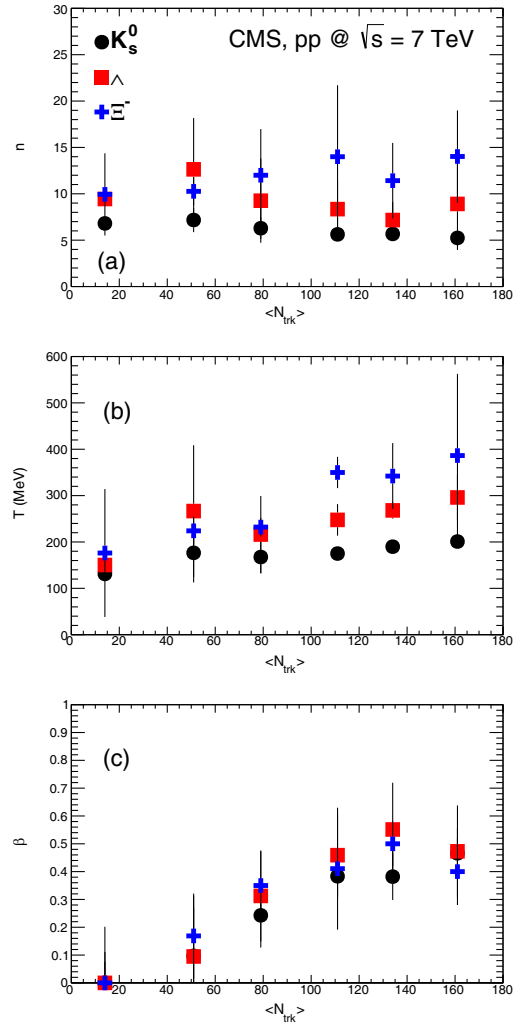


**Fig. 2.** The Tsallis parameters  $n$ ,  $T$  and  $\beta$  for the strange hadrons as a function of mean track multiplicity  $\langle N_{\text{trk}} \rangle$  of event class in pp collision at  $\sqrt{s} = 7$  TeV.

which can be inferred from the values of  $\chi^2/\text{NDF}$  given in table 1.

Figure 2(a) shows the Tsallis parameter  $n$  for the strange hadrons  $K_s^0$ ,  $\Lambda$  and  $\Xi^-$  as a function of event multiplicity in the pp collisions at  $\sqrt{s} = 7$  TeV. The parameters  $T$  and  $\beta$  are shown in panels (b) and (c), respectively.

**Table 2.**  $\chi^2/\text{NDF}$  of the strange hadrons production in pPb collision at  $\sqrt{s_{NN}} = 5.02$  TeV obtained using individual fitting.

$\langle N_{\text{trk}} \rangle$	$\chi^2/\text{NDF}$		
	$K_s^0$	$\Lambda$	$\Xi^-$
21	0.043	0.029	0.058
57	0.019	0.023	0.058
89	0.021	0.015	0.044
125	0.023	0.020	0.111
159	0.015	0.026	0.067
195	0.016	0.019	0.043
236	0.017	0.021	0.048
280	0.017	0.025	0.077

The value of  $n$  increases with the mass of particles but there is little variation with multiplicity. It means that the degree of thermalization remains similar for the events of different multiplicity classes. The value of Tsallis temperature  $T$  increases with the multiplicity for all three hadrons and becomes large for the highest multiplicity events. The transverse flow also increases with multiplicity for all the three hadrons. The highest value of  $\beta$  remains in the range 0.4–0.5 in pp system.

Figure 3 shows the invariant yields of  $K_s^0$ ,  $\Lambda$  and  $\Xi^-$  as a function of  $p_T$  in panels (a), (b) and (c), respectively, for pPb collisions at  $\sqrt{s_{NN}} = 5.02$  TeV measured by the CMS experiment [33]. The invariant yields are given for eight multiplicity classes which correspond to the efficiency corrected average track multiplicities  $\langle N_{\text{trk}} \rangle = 21, 57, 89, 125, 159, 195, 236$  and  $280$  [34]. The solid curves are the modified Tsallis distributions fitted individually to different hadron spectra. The individual fitting gives excellent fit quality for all the multiplicity classes which can be seen from the values of  $\chi^2/\text{NDF}$  given in table 2.

Figure 4(a) shows the Tsallis parameter  $n$  for the strange hadrons  $K_s^0$ ,  $\Lambda$  and  $\Xi^-$  as a function of event multiplicity in the pPb collisions at  $\sqrt{s_{NN}} = 5.02$  TeV. The parameters  $T$  and  $\beta$  are shown in panels (b) and (c), respectively. Like pp system, similar conclusions can be drawn for the pPb system. The degree of thermalization remains similar for the events of different multiplicity classes. The value of Tsallis temperature  $T$  increases with the multiplicity for all three hadrons and becomes large for the highest multiplicity events. The transverse flow also increases with multiplicity for all the three hadrons. The highest value of  $\beta$  remains in the range 0.4–0.5 for  $K_s^0$  and  $\Lambda$  and 0.75–0.85 for  $\Xi^-$  in pPb system.

Figure 5 shows the invariant yields of  $K_s^0$ ,  $\Lambda$  and  $\Xi^-$  as a function of  $p_T$  in panels (a), (b) and (c), respectively, for PbPb collisions at  $\sqrt{s_{NN}} = 2.76$  TeV measured by the CMS experiment [33]. The invariant yields are given for eight multiplicity classes which correspond to the average efficiency corrected track multiplicities  $\langle N_{\text{trk}} \rangle = 21, 58, 92, 130, 168, 210, 253$  and  $299$  [34]. The solid curves are the modified Tsallis distributions fitted individually to different hadron spectra. The individual fitting gives

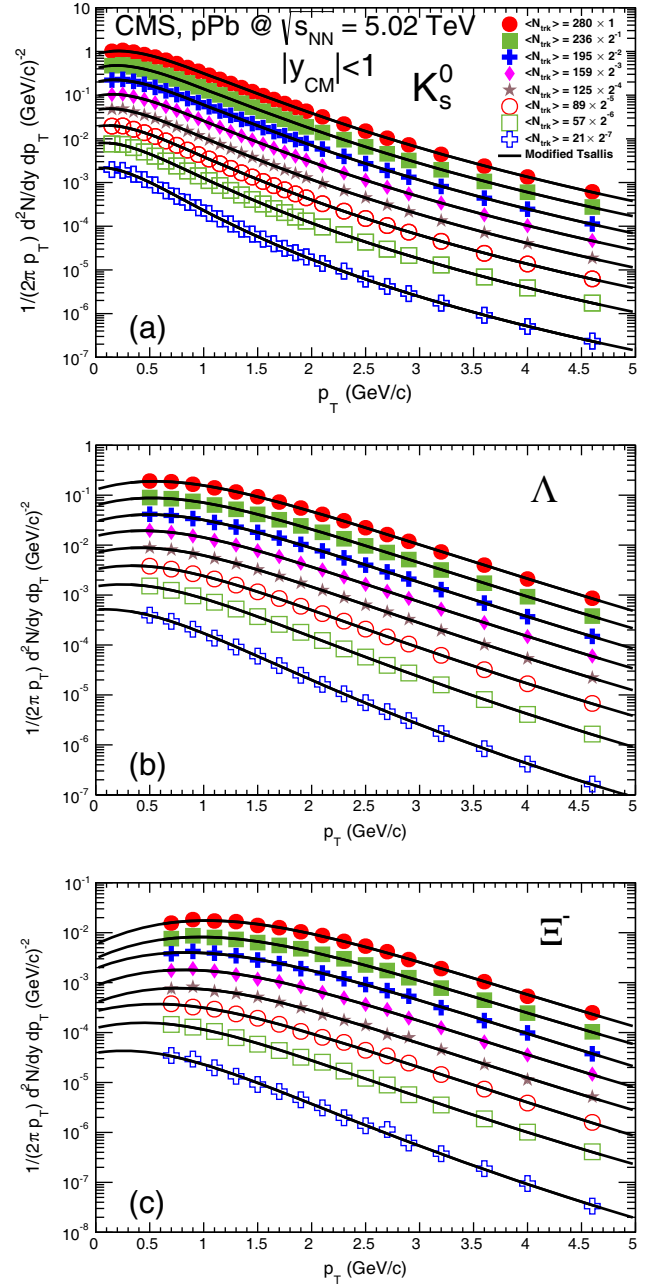


**Fig. 3.** The invariant yields of the  $K_s^0$ ,  $\Lambda$  and  $\Xi^-$  hadrons as a function of the transverse momentum  $p_T$  for pPb collisions at  $\sqrt{s_{NN}} = 5.02$  TeV measured by CMS [33]. The yields are shown for different multiplicity bins. The solid curves are the fitted modified Tsallis distribution.

excellent fit quality for all the multiplicity classes which can be seen from the values of  $\chi^2/\text{NDF}$  given in table 3.

Figure 6(a) shows the Tsallis parameter  $n$  for the strange hadrons  $K_s^0$ ,  $\Lambda$  and  $\Xi^-$  as a function of event multiplicity in the PbPb collisions at  $\sqrt{s_{NN}} = 2.76$  TeV. The parameters  $T$  and  $\beta$  are shown in panels (b) and (c), respectively. The degree of thermalization remains similar for the events of different multiplicity classes of PbPb collisions. Unlike pp and pPb systems, the value of Tsallis

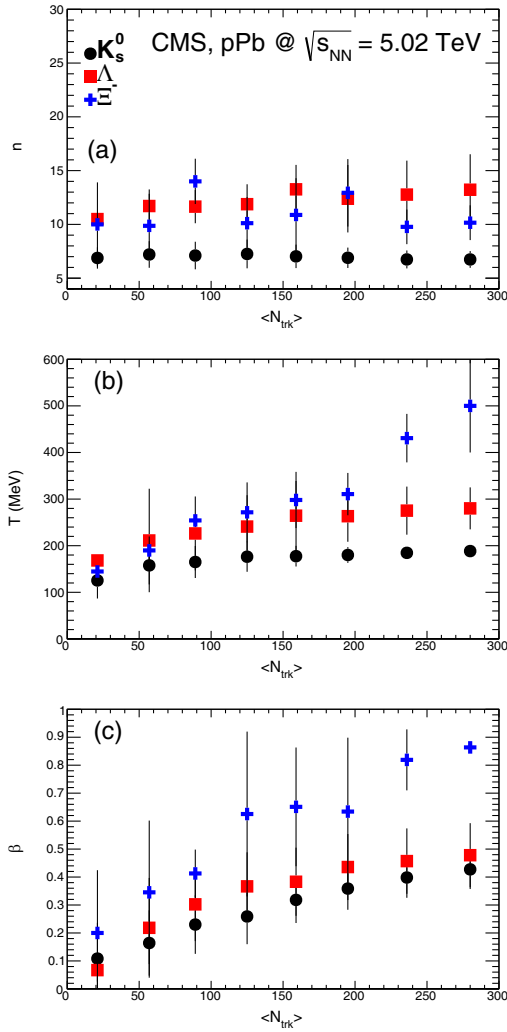


**Fig. 4.** The Tsallis parameters  $n$ ,  $T$  and  $\beta$  for the strange hadrons as a function of mean track multiplicity  $\langle N_{\text{trk}} \rangle$  in pPb collision at  $\sqrt{s_{NN}} = 5.02$  TeV.

temperature  $T$  varies little with the multiplicity for all three hadrons. The transverse flow  $\beta$  also increases with multiplicity for all the three hadrons. The highest value of  $\beta$  remains in the range 0.3–0.4 for  $K_s^0$  and  $\Lambda$  and 0.75–0.85 for  $\Xi^-$  in PbPb system.

We have studied the spectra in the three systems pp, pPb and PbPb. Since all the three systems are at different collision energy, they cannot be compared directly. Moreover, how the multiplicity class can be related to the system size is not clear. For PbPb system, the highest multiplicity class presented corresponds to a centrality class of 55%, which can be called semi-peripheral events. It is still possible to draw some general trends from the present analysis. The behaviour of various parameters like  $n$  and  $\beta$  with the event multiplicity are similar for the three systems. The Tsallis temperature  $T$  increases with the multiplicity for pp and pPb systems but it does not show a noticeable change with the event multiplicity for the PbPb system. The PbPb system has smaller temperature and

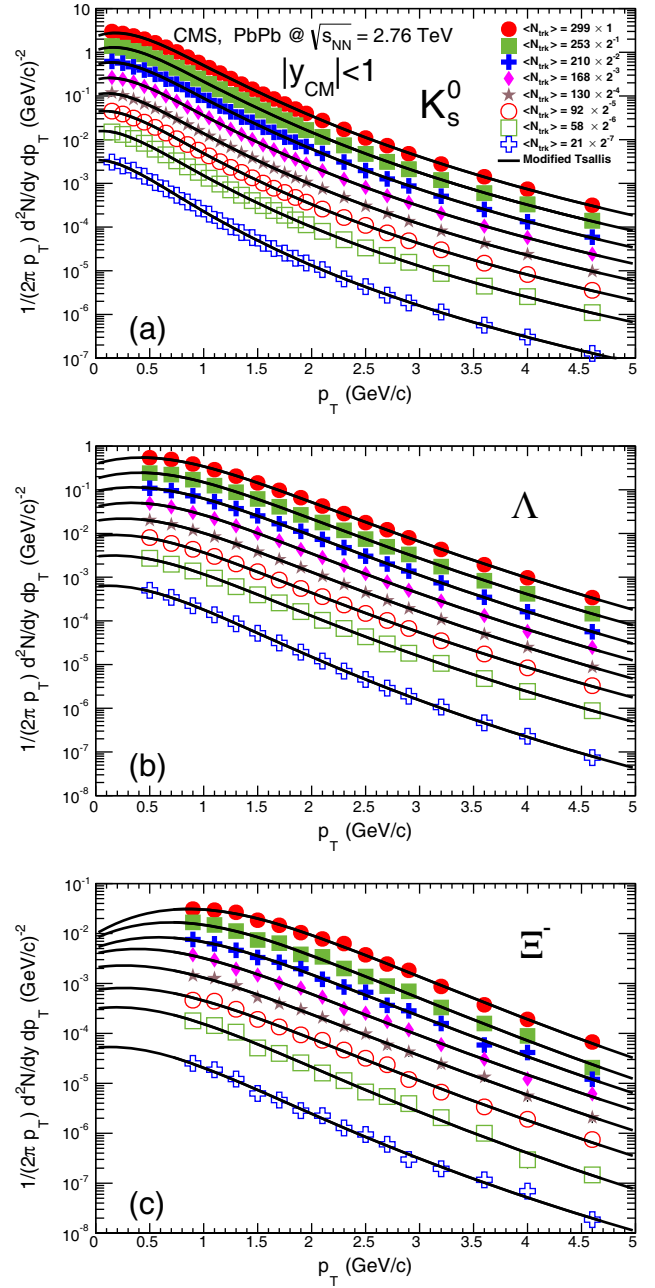


**Fig. 5.** The invariant yields of the  $K_s^0$ ,  $\Lambda$  and  $\Xi^-$  hadrons as a function of the transverse momentum  $p_T$  for PbPb collisions at  $\sqrt{s_{NN}} = 2.76$  TeV measured by CMS [33]. The yields are shown for different multiplicity bins. The solid curves are the fitted modified Tsallis distribution.

transverse flow as compared to the pp and pPb systems. The PbPb system being large will maintain collectivity for longer time and hence freeze-out at lower temperature.

We also carry out the above study using a single freeze-out scenario for all the hadrons. It is possible to find out same set of parameters corresponding to a good fit using combined fitting of the three hadron spectra. The combined fitting is performed in the  $p_T$  range 0.3–3.8 GeV for  $K_s^0$ , 0.6–3.8 GeV for  $\Lambda$  and 1.2–3.8 GeV for  $\Xi^-$ . The  $p_T$

**Table 3.**  $\chi^2/\text{NDF}$  of the strange hadrons production in PbPb collision at  $\sqrt{s_{NN}} = 2.76$  TeV obtained using individual fitting.

$\langle N_{\text{trk}} \rangle$	$\chi^2/\text{NDF}$		
	$K_s^0$	$\Lambda$	$\Xi^-$
21	0.034	0.109	0.407
58	0.024	0.069	0.507
92	0.033	0.077	0.387
130	0.068	0.029	0.204
168	0.023	0.185	0.249
210	0.063	0.028	0.285
253	0.068	0.056	0.336
299	0.080	0.059	0.179

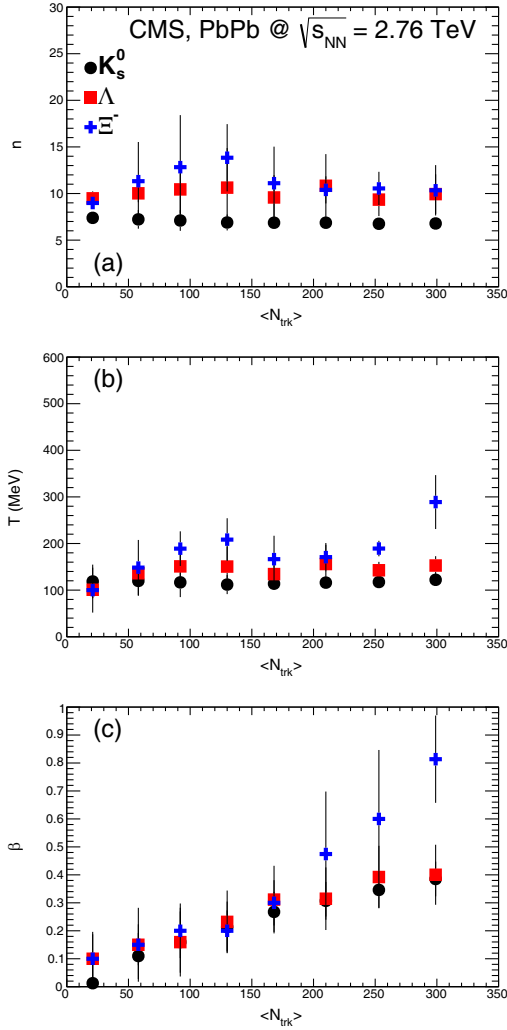


**Fig. 6.** The Tsallis parameters  $n$ ,  $T$  and  $\beta$  for the strange hadrons as a function of mean track multiplicity  $\langle N_{\text{trk}} \rangle$  in PbPb collision at  $\sqrt{s_{NN}} = 2.76$  TeV.

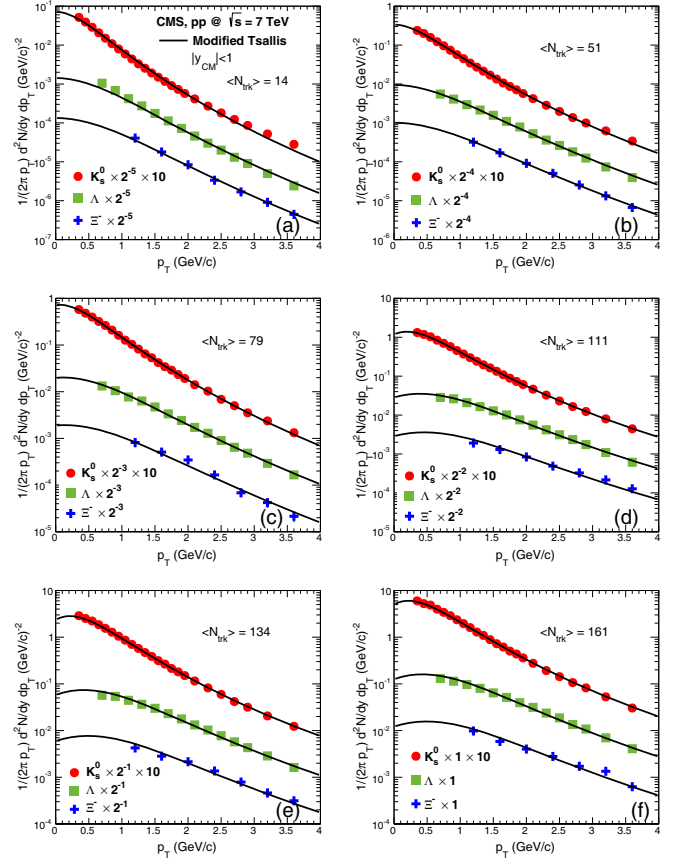


**Fig. 7.** The invariant yields of the  $K_s^0$ ,  $\Lambda$  and  $\Xi^-$  hadrons as a function of the transverse momentum ( $p_T$ ) for pp collisions at  $\sqrt{s} = 7$  TeV measured by CMS [33]. Each panel corresponds to a different event multiplicity class. The solid curves are the fitted modified Tsallis distribution.

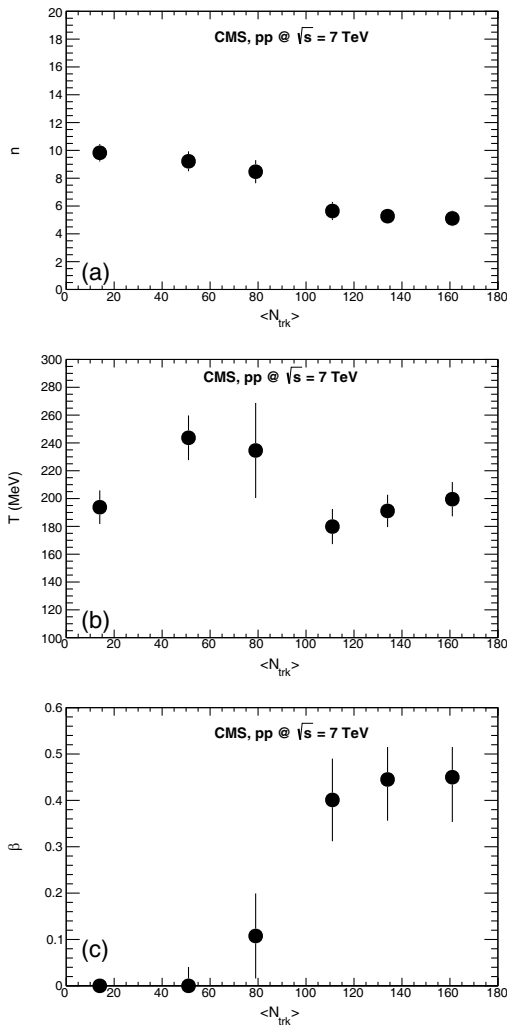
range for all the particle spectra is kept same over the three systems.

Figure 7 shows the invariant yields of strange hadrons  $K_s^0$  (red circle),  $\Lambda$  (green square) and  $\Xi^-$  (blue cross) as a function of  $p_T$  for pp collisions at  $\sqrt{s} = 7$  TeV measured by CMS experiment [33] for average track multiplicities  $\langle N_{\text{trk}} \rangle = 14$  (panel (a)), 51 (panel (b)), 79 (panel (c)), 111 (panel (d)), 134 (panel (e)) and 161 (panel (f)). The solid curves are the modified Tsallis distributions fitted simultaneously to the three hadron spectra for a given multiplicity class. While the fit quality in individual fitting was better, the combined fitting gives reasonable quality fits for all multiplicity classes (except for the lowest multiplicity class) which can be judged from the values of  $\chi^2/\text{NDF}$  given in table 4.

Figure 8(a) shows the Tsallis parameter  $n$  obtained from combined fitting of three strange hadrons as a function of the event multiplicity in the pp collision at  $\sqrt{s} = 7$  TeV. The parameters  $T$  and  $\beta$  are shown in panels (b) and (c), respectively. It can be seen from the figure that  $n$  decreases with multiplicity and its value becomes  $\sim 5$  for the high multiplicity classes. The temperature  $T$  does not show any trend with increasing multiplicity but it increases smoothly in the three highest multiplicity bins.

**Table 4.**  $\chi^2/\text{NDF}$  of the strange hadrons production in pp collision at  $\sqrt{s} = 7$  TeV, pPb collision at  $\sqrt{s_{NN}} = 5.02$  TeV and PbPb collisions at  $\sqrt{s_{NN}} = 2.76$  TeV obtained using combined fitting.

pp		pPb		PbPb	
$\langle N_{\text{trk}} \rangle$	$\frac{\chi^2}{\text{NDF}}$	$\langle N_{\text{trk}} \rangle$	$\frac{\chi^2}{\text{NDF}}$	$\langle N_{\text{trk}} \rangle$	$\frac{\chi^2}{\text{NDF}}$
14	1.989	21	1.035	21	1.954
51	0.308	57	1.559	58	0.847
79	0.261	89	0.202	92	0.668
111	0.262	125	0.223	130	0.504
134	0.385	159	0.348	168	0.464
161	0.362	195	0.454	210	0.446
–	–	236	0.688	253	0.421
–	–	280	0.833	299	0.509



**Fig. 8.** The Tsallis parameters  $n$ ,  $T$  and  $\beta$  for the strange hadrons as a function of mean track multiplicity  $\langle N_{\text{trk}} \rangle$  in pp collision at  $\sqrt{s} = 7$  TeV.

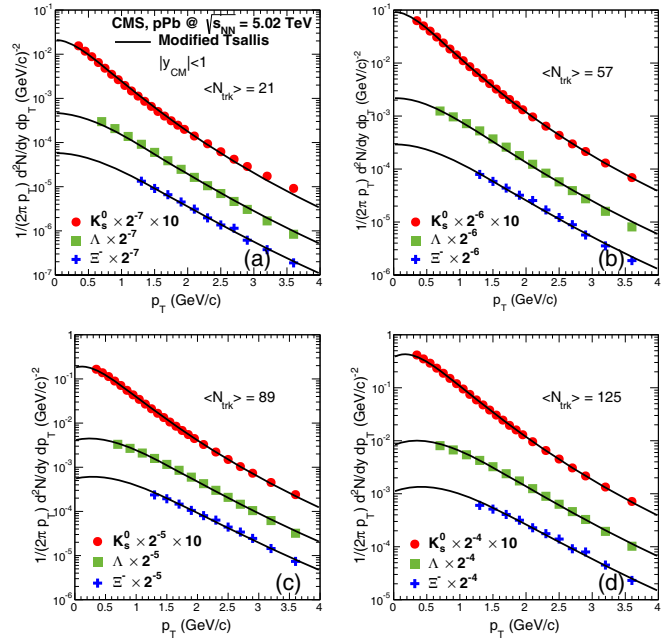


**Fig. 9.** The invariant yields of the  $K_s^0$ ,  $\Lambda$  and  $\Xi^-$  hadrons as a function of the transverse momentum  $p_T$  for pPb collisions at  $\sqrt{s_{NN}} = 5.02$  TeV measured by CMS [33]. Different panels correspond to different multiplicity bins. The solid curves are the fitted modified Tsallis distribution.

The transverse flow  $\beta$  is zero for the first two multiplicity bins and then sharply increases up to 0.5 in the three highest multiplicity bins.

Figure 9 shows the invariant yields of strange hadrons  $K_s^0$ ,  $\Lambda$  and  $\Xi^-$  as a function of  $p_T$  for pPb collisions at  $\sqrt{s_{NN}} = 5.02$  TeV measured by CMS experiment [33] for the average track multiplicities  $\langle N_{\text{trk}} \rangle = 21$  (panel (a)), 57 (panel (b)), 89 (panel (c)) and 125 (panel (d)). Figure 10 corresponds to average track multiplicities  $\langle N_{\text{trk}} \rangle = 159$  (panel (a)), 195 (panel (b)), 236 (panel (c)) and 280 (panel (d)) in pPb collisions. In both the figures, the solid curves are the modified Tsallis distributions fitted simultaneously to the three strange hadrons. The fit quality is reasonably good except for the two lowest multiplicity classes which can be judged from the values of  $\chi^2/\text{NDF}$  given in table 4.

Figure 11(a) shows the Tsallis parameter  $n$  obtained from combined fitting of three strange hadrons as a function of the event multiplicity in the pPb collision at  $\sqrt{s_{NN}} = 5.02$  TeV. The parameters  $T$  and  $\beta$  are shown in panels (b) and (c), respectively. Like pp system, in pPb system also  $n$  decreases with multiplicity and its value becomes  $\sim 6$  for the high multiplicity classes. The temperature  $T$  smoothly decreases with multiplicity for the first few bins, then increases slightly in the last four most central bins. The transverse flow  $\beta$  increases with the event multiplicity and roughly saturates at 0.5 for the largest multiplicity bins. On comparing figs. 8 and 11 one can conclude that the values of parameters and their behaviour are the same if we pick up the same track classes of the pp and pPb systems.

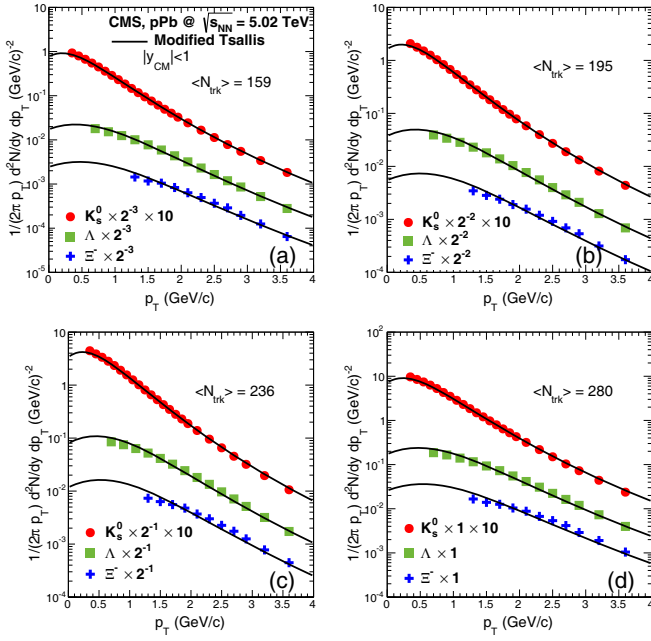


**Fig. 10.** The invariant yields of the  $K_s^0$ ,  $\Lambda$  and  $\Xi^-$  hadrons as a function of the transverse momentum  $p_T$  for pPb collisions at  $\sqrt{s_{NN}} = 5.02$  TeV measured by CMS [33]. Different panels correspond to different multiplicity bins. The solid curves are the fitted modified Tsallis distribution.

Figure 12 shows the invariant yields of strange hadrons  $K_s^0$ ,  $\Lambda$  and  $\Xi^-$  as a function of  $p_T$  for PbPb collisions at  $\sqrt{s_{NN}} = 2.76$  TeV measured by CMS experiment [33] for average track multiplicities  $\langle N_{\text{trk}} \rangle = 21$  (panel (a)), 58 (panel (b)), 92 (panel (c)) and 130 (panel (d)). Figure 13 corresponds to average track multiplicities  $\langle N_{\text{trk}} \rangle = 168$  (panel (a)), 210 (panel (b)), 253 (panel (c)) and 299 (panel (d)). In both the figures the solid curves are the modified Tsallis distributions fitted simultaneously to three strange hadrons. The fit quality is reasonably good except for the lowest multiplicity classes which can be judged from the values of  $\chi^2/\text{NDF}$  given in table 4.

Figure 14(a) shows the Tsallis parameter  $n$  obtained from combined fitting of three strange hadrons as a function of the event multiplicity in the PbPb collision at  $\sqrt{s_{NN}} = 2.76$  TeV. The parameters  $T$  and  $\beta$  are shown in panels (b) and (c), respectively. The PbPb system looks different from the pp and pPb systems. The value of parameter  $n$  shows a slight increase with the multiplicity and has a higher value ( $\sim 12$ ) as compared to that for smaller systems. The temperature  $T$  smoothly increases with multiplicity for the first few bins then decreases smoothly in the last four most central bins, which is a trend opposite to what is found in the pPb collisions. The transverse flow velocity  $\beta$  remains zero for the first five multiplicity classes and increases up to 0.2 for the highest multiplicity class. The transverse flow in PbPb system remains lower as compared to pp and pPb systems. The highest multiplicity class of the PbPb system corresponds to a semi-peripheral collision and we expect that for central collisions the value of  $\beta$  will become large.

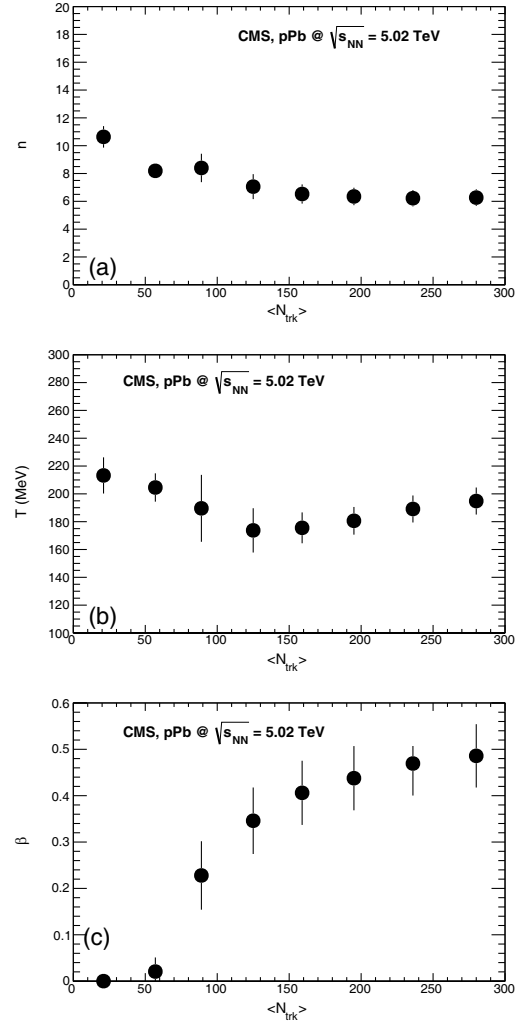


**Fig. 11.** The Tsallis parameters  $n$ ,  $T$  and  $\beta$  for the strange hadrons as a function of mean track multiplicity  $\langle N_{\text{trk}} \rangle$  in pPb collision at  $\sqrt{s_{NN}} = 5.02$  TeV.

## 4 Conclusion

We carried out an analysis of transverse momentum spectra of the strange hadrons in different multiplicity events produced in pp collision at  $\sqrt{s} = 7$  TeV, pPb collision at  $\sqrt{s_{NN}} = 5.02$  TeV and PbPb collision at  $\sqrt{s_{NN}} = 2.76$  TeV using Tsallis distribution modified to include transverse flow. The analysis is performed for both the differential and single freeze-out scenarios of the strange hadrons  $K_s^0$ ,  $\Lambda$  and  $\Xi^-$ . In both freeze-out scenarios, the transverse flow increases with event multiplicity for all the three systems.

In the case of the differential freeze-out scenario, the value of parameter  $n$  has a little variation with multiplicity implying that the degree of thermalization remains similar for the events of different multiplicity classes in all the three systems. For the differential freeze-out scenario the value of Tsallis temperature increases with the mass of the hadrons and also increases with the multiplicity of the event class in pp and pPb system. In PbPb system, the



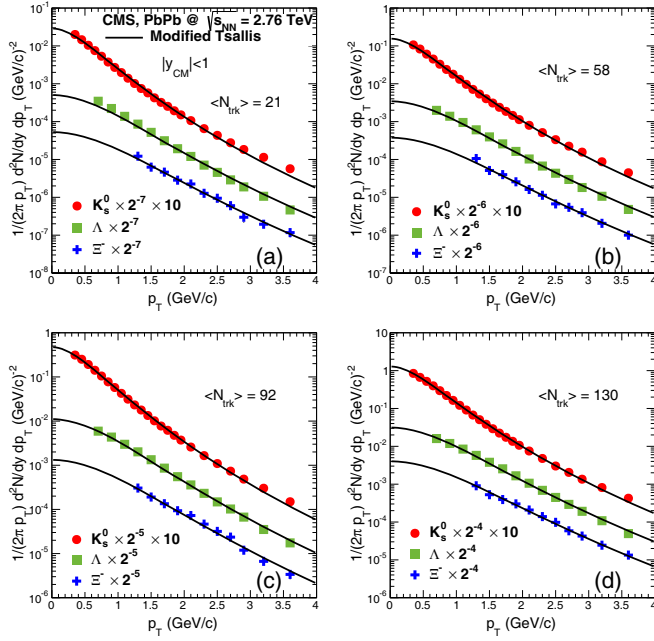


**Fig. 12.** The invariant yields of the  $K_s^0$ ,  $\Lambda$  and  $\Xi^-$  hadrons as a function of the transverse momentum  $p_T$  for PbPb collisions at  $\sqrt{s_{NN}} = 2.76$  TeV measured by CMS [33]. Different panels correspond to different multiplicity bins. The solid curves are the fitted modified Tsallis distribution.

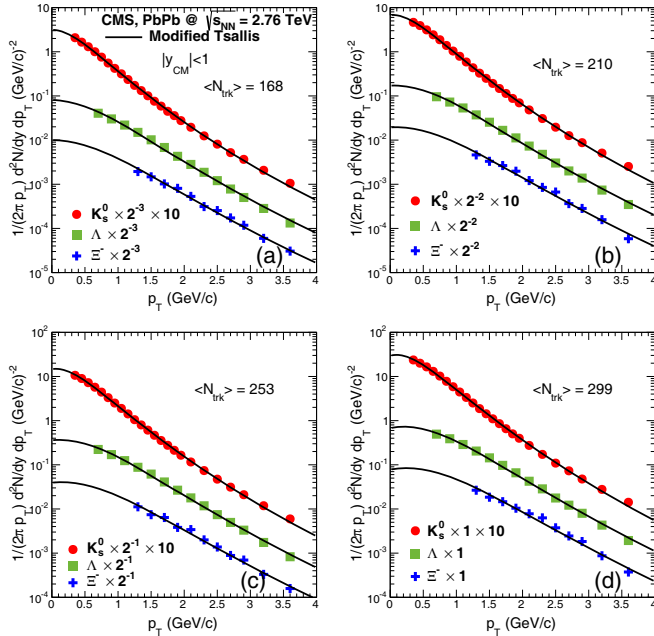


**Fig. 13.** The invariant yields of the  $K_s^0$ ,  $\Lambda$  and  $\Xi^-$  hadrons as a function of the transverse momentum  $p_T$  for PbPb collisions at  $\sqrt{s_{NN}} = 2.76$  TeV measured by CMS [33]. Different panels correspond to different multiplicity bins. The solid curves are the fitted modified Tsallis distribution.

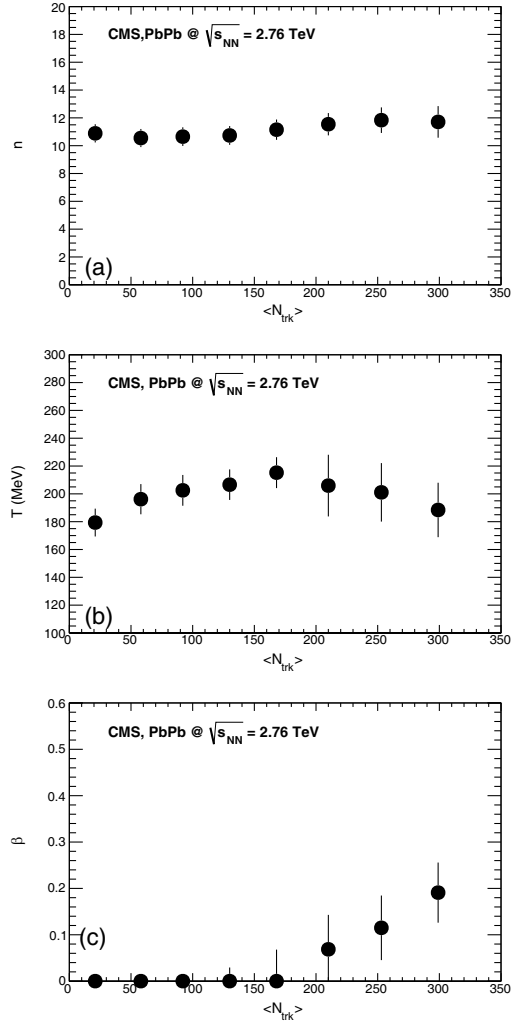


**Fig. 14.** The Tsallis parameters  $n$ ,  $T$  and  $\beta$  for the strange hadrons as a function of mean track multiplicity  $\langle N_{\text{trk}} \rangle$  in PbPb collision at  $\sqrt{s_{NN}} = 2.76$  TeV.

value of Tsallis temperature shows little variation with the multiplicity for all the three hadrons.

In the case of the single freeze-out scenario the difference between small systems (pp, pPb) and PbPb system becomes more evident. For pp and pPb systems, the parameter  $n$  decreases with increasing multiplicity but for PbPb system it shows a slight increase with the multiplicity and has a larger value as compared to that for smaller systems. For single freeze-out scenario, the temperature in PbPb system smoothly increases with multiplicity for the first few bins then smoothly decreases which is a trend opposite to what is found in the pp and pPb systems. It is expected that if a truly collective system is formed, the temperature decreases or remains constant as the system size increases. Decreasing temperature for PbPb system above  $N_{\text{trk}} = 150$  is indicative of that.

We are thankful to CMS publication committee for providing the tables of the published data.

## References

1. J.D. Bjorken, Phys. Rev. D **27**, 140 (1983).
2. T. Ullrich, B. Wyslouch, J.W. Harris, Nucl. Phys. A **904-905**, 1c (2013).
3. M. Gyulassy, L. McLerran, Nucl. Phys. A **750**, 30 (2005) arXiv:nucl-th/0405013.
4. T. Hirano, Y. Nara, Phys. Rev. C **69**, 034908 (2004) arXiv:nucl-th/0307015.
5. R.J. Fries, V. Greco, P. Sorensen, Annu. Rev. Nucl. Part. Sci. **58**, 177 (2008) arXiv:0807.4939 [nucl-th].
6. B. Mller, Phys. Scripta T **158**, 014004 (2013) arXiv:1309.7616 [nucl-th].
7. W. Li, Mod. Phys. Lett. A **27**, 1230018 (2012) arXiv:1206.0148 [nucl-ex].
8. CMS Collaboration (V. Khachatryan *et al.*), JHEP **09**, 091 (2010) arXiv:1009.4122 [hep-ex].
9. P. Ghosh, S. Muhuri, J.K. Nayak, R. Varma, J. Phys. G **41**, 035106 (2014).
10. C. Tsallis, J. Stat. Phys. **52**, 479 (1988).
11. T.S. Biro, G. Purcsel, K. Urmosy, Eur. Phys. J. A **40**, 325 (2009) arXiv:0812.2104 [hep-ph].
12. P.K. Khandai, P. Sett, P. Shukla, V. Singh, Int. J. Mod. Phys. A **28**, 1350066 (2013) arXiv:1304.6224 [hep-ph].
13. C.Y. Wong, G. Wilk, Phys. Rev. D **87**, 114007 (2013) arXiv:1305.2627 [hep-ph].
14. R. Hagedorn, Riv. Nuovo Cimento **6**, N.10 (1983).
15. R. Blankenbecler, S.J. Brodsky, Phys. Rev. D **10**, 2973 (1974).
16. PHENIX Collaboration (A. Adare *et al.*), Phys. Rev. D **83**, 052004 (2011) arXiv:1005.3674 [hep-ex].
17. P. Sett, P. Shukla, Adv. High Energy Phys. **2014**, 896037 (2014) arXiv:1408.1034 [hep-ph].
18. Z. Tang, Y. Xu, L. Ruan, G. van Buren, F. Wang, Z. Xu, Phys. Rev. C **79**, 051901 (2009) arXiv:0812.1609 [nucl-ex].
19. P.K. Khandai, P. Sett, P. Shukla, V. Singh, J. Phys. G **41**, 025105 (2014) arXiv:1310.4022 [nucl-th].
20. P. Sett, P. Shukla, Int. J. Mod. Phys. E **24**, 1550046 (2015) arXiv:1505.05258 [hep-ph].
21. H. Zheng, L. Zhu, A. Bonasera, Phys. Rev. D **92**, 074009 (2015) arXiv:1506.03156 [nucl-th].
22. ALICE Collaboration (B. Abelev *et al.*), Phys. Rev. C **88**, 044910 (2013) arXiv:1303.0737 [hep-ex].
23. D. Thakur, S. Tripathy, P. Garg, R. Sahoo, J. Cleymans, arXiv:1601.05223 [hep-ph].
24. H.L. Lao, H.R. Wei, F.H. Liu, R.A. Lacey, Eur. Phys. J. A **52**, 203 (2016) arXiv:1601.00045 [nucl-th].
25. H.R. Wei, F.H. Liu, R.A. Lacey, Eur. Phys. J. A **52**, 102 (2016) arXiv:1601.07045 [hep-ph].
26. G. Wilk, Z. Wlodarczyk, Phys. Rev. Lett. **84**, 2770 (2000) arXiv:hep-ph/9908459.
27. J. Cleymans, D. Worku, Eur. Phys. J. A **48**, 160 (2012) arXiv:1203.4343 [hep-ph].
28. PHENIX Collaboration (A. Adare *et al.*), Phys. Rev. C **83**, 064903 (2011) arXiv:1102.0753 [nucl-ex].
29. STAR Collaboration (B.I. Abelev *et al.*), Phys. Rev. C **75**, 064901 (2007) arXiv:nucl-ex/0607033.
30. R. Blankenbecler, S.J. Brodsky, J.F. Gunion, Phys. Rev. D **12**, 3469 (1975).
31. S.J. Brodsky, H.J. Pirner, J. Raufeisen, Phys. Lett. B **637**, 58 (2006) arXiv:hep-ph/0510315.
32. J. Cleymans, G. Hamar, P. Levai, S. Wheaton, J. Phys. G **36**, 064018 (2009) arXiv:0812.1471 [hep-ph].
33. CMS Collaboration (V. Khachatryan *et al.*), arXiv:1605.06699 [nucl-ex].
34. CMS Collaboration (S. Chatrchyan *et al.*), Phys. Lett. B **724**, 213 (2013) arXiv:1305.0609 [nucl-ex].